

OPEN

# Two Distinct Types of Sweat Profile in Healthy Subjects While Exercising at Constant Power Output Measured by a Wearable Sweat Sensor

Dong-Hoon Choi<sup>1</sup>, Grant Kitchen<sup>1</sup>, Ji Soo Kim<sup>2</sup>, Yi Li<sup>1</sup>, Kain Kim<sup>1</sup>, In cheol Jeong<sup>1</sup>, Jane Nguyen<sup>1</sup>, Kerry J. Stewart<sup>3</sup>, Scott L. Zeger<sup>2</sup> & Peter C. Se arson<sup>1,4,\*</sup>

Wearable sweat sensors have enabled real-time monitoring of sweat profiles (sweat concentration versus time) and could enable monitoring of electrolyte loss during exercise or for individuals working in extreme environments. To assess the feasibility of using a wearable sweat chloride sensor for real-time monitoring of individuals during exercise, we recorded and analyzed the sweat profiles of 50 healthy subjects while spinning at 75 Watts for 1 hour. The measured sweat chloride concentrations were in the range from 2.9–34 mM. The sweat profiles showed two distinct sweat responses: Type 1 (single plateau) and Type 2 (multiple plateaus). Subjects with Type 2 profiles had higher sweat chloride concentration and weight loss, higher maximum heart rate, and larger changes in heart rate and rating of perceived exertion during the trial compared to subjects with Type 1 profiles. To assess the influence of level of effort, we recorded sweat profiles for five subjects at 75W, 100W, and 125W. While all five subjects showed Type 1 sweat profiles at 75W, four of the subjects had Type 2 profiles at 125W, showing an increase in sweat chloride with exercise intensity. Finally, we show that sweat profiles along with other physiological parameters can be used to predict fluid loss.

Secretion of fluid by sweat glands in the skin can occur in response to various thermal and chemical stimuli. Sweat contains sodium, potassium, and chloride ions and hence sweating is directly coupled with changes in electrolyte balance in the body. In healthy individuals, the electrolyte and water loss during sweating can lead to a range of conditions, such as hypo- and hypernatremia. Exercise performance is also influenced by electrolyte loss and dehydration<sup>1–6</sup>. Furthermore, working in hot environments with poor hydration has been linked to chronic kidney disease<sup>7,8</sup>. The recent development of wearable sweat sensors<sup>9–18</sup> provides new opportunities to study fundamental issues associated with electrolyte loss in health and disease, enabling real-time measurement of the dynamic response outside of the laboratory. Previous studies have largely relied on laboratory analysis of samples collected during a trial<sup>19–21</sup>, which precludes real-time analysis. From a health and fitness perspective, wearable sweat sensors provide real time data that could be used to prevent heat-related injury and optimize athletic performance<sup>22–24</sup>.

Sweating is complex thermoregulation process that is dependent on physiological responses including cardiovascular function, skin and core temperature responses, plasma volume, and sweat rate<sup>25–27</sup>. Wearable technologies have the potential to contribute to the understanding of sweating, and to develop tools to predict and prevent heat-related injuries. In previous work we have developed a wearable sweat sensor<sup>9–11</sup> and have validated sensor performance in studies with healthy subjects and individuals with CF following chemically induced sweating<sup>10</sup>. Here, building on our previous work, we make three key advances. First, to demonstrate the potential for

<sup>1</sup>Institute for Nanobiotechnology, Johns Hopkins University, 3400 North Charles Street, Baltimore, Maryland, 21218, USA. <sup>2</sup>Department of Biostatistics, Johns Hopkins University, 615 North Wolfe Street, Baltimore, Maryland, 21205, USA. <sup>3</sup>Department of Medicine, Johns Hopkins University School of Medicine, 4940 Eastern Ave, Baltimore, Maryland, 21224, USA. <sup>4</sup>Department of Materials Science and Engineering, 3400 North Charles Street, Baltimore, Maryland, 21218, USA. \*email: [searson@jhu.edu](mailto:searson@jhu.edu)

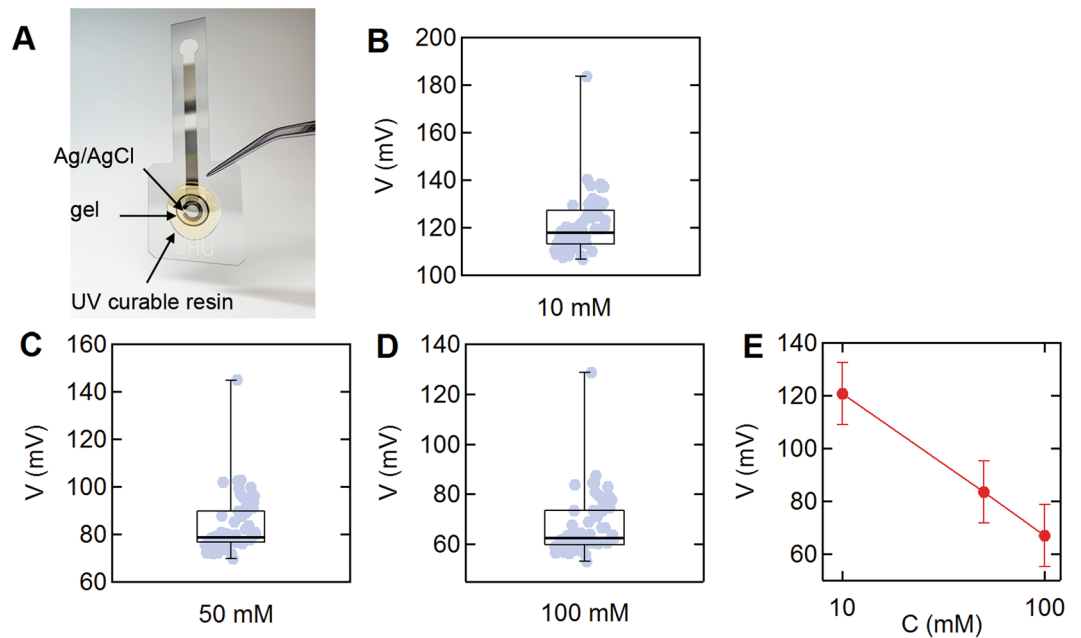


**Figure 1.** Wearable sweat chloride sensor. (A) Photograph of the potentiometric sweat sensor. (B–D) Distribution of sensor voltages in (B) 10 mM, (C) 50 mM, and 100 mM NaCl solutions ( $N = 65$ ). Box and whisker plots display the minimum, first quartile, median, third quartile, and maximum values. (E) Average calibration curve obtained from the 65 sensors used in this study.

real-time measurement during exercise, we performed on-body trials with 50 healthy subjects while spinning on an exercise bike at 75 W for 60 minutes. To assess the link between the sweat profile and other physiological parameters, we simultaneously monitored heart rate, core temperature, skin temperature, and the rating of perceived exertion (RPE), along with overall weight loss. Second, we classified the 50 subjects into two groups based on their sweat profiles and assessed the relationship between the sweat profiles and other physiological responses. To assess the influence of level of effort on sweat profile, we performed trials with five subjects at 75, 100, and 125 W for 1 hour. Third, using machine learning, we showed how the physiological data measured during exercise can be used to predict risk for dehydration due to excessive fluid loss.

## Results and Discussion

**Wearable sweat chloride sensor.** All trials were performed using a wearable potentiometric sweat chloride sensor developed in our lab (Fig. 1A)<sup>10,11</sup>. We used a total of 65 sensors to record sweat profiles, and all sensors were calibrated prior to each trial. The voltages of 65 devices in 10, 50, and 100 mM of three standard sodium chloride (NaCl) solutions were  $120.8 \pm 11.8$ ,  $83.4 \pm 11.8$  and  $67.1 \pm 11.8$  mV (mean  $\pm$  SD) mV, respectively (Fig. 1B–D). The slope and y-intercept of the calibration values obtained from the voltages were  $-53.6 \pm 3.5$  (mean  $\pm$  SD (standard deviation)) mV/decade and  $174.4 \pm 12.9$  (SD) mV, respectively (Fig. 1E). If the average calibration curve was used for the standard measurements, the error in the 10, 50, and 100 mM solutions was  $1.0 \pm 4.0$ ,  $4.7 \pm 19.1$ , and  $10.2 \pm 38.1$  mM (mean  $\pm$  SD), respectively.

**Variation of the sweat chloride concentration among healthy subjects.** 50 healthy individuals were recruited to spin at a constant power output of 75 W for 60 minutes following a 25 minute warm-up (Fig. S1 in Supplementary Information). Figure 2 shows the setup of the trial in this study. During the trials, the sweat chloride concentration was wirelessly monitored using a Bluetooth transceiver and mobile app with a 1 Hz sampling rate. The heart rate was also wirelessly monitored at a 1 Hz sampling rate, and a thermocouple sensor was used to monitor skin temperature at a 2 Hz sampling rate. The core temperature and RPE were manually recorded every 5 minutes, and the overall weight change was obtained by measuring the subject's weight before and after the trial.

The exercise protocol and the results from a typical trial are shown in Fig. 3A–F. Within a few minutes of the onset of sweating, typically at the end of the warm-up period (25 minutes), the sweat chloride concentration reached a plateau of about 5 mM (Fig. 3B). The initial transient response before reaching the plateau is due to the high sensor impedance caused by insufficient sweat and does not reflect a high sweat chloride concentration. Here we define a plateau region as a period where the slope of the sweat profile was smaller than  $0.1 \text{ mM min}^{-1}$  for at least 10 minutes. The heart rate remained at about 120 bpm and the RPE was about 12 during the 60 minutes at 75 W (Fig. 3C,D). The core temperature and skin temperature were also constant during the trial, with values of  $36.5^\circ\text{C}$  and  $32^\circ\text{C}$ , respectively (Fig. 3E,F). Skin temperatures are typically  $3\text{--}4^\circ\text{C}$  lower than the core temperature under thermoneutral ambient conditions<sup>28</sup>.

The onset of sweating, determined from the change in noise level of the measured sweat concentration, generally occurred during the warm-up period ( $15.1 \pm 7.5$  minutes; mean  $\pm$  CI (95% confidence interval))

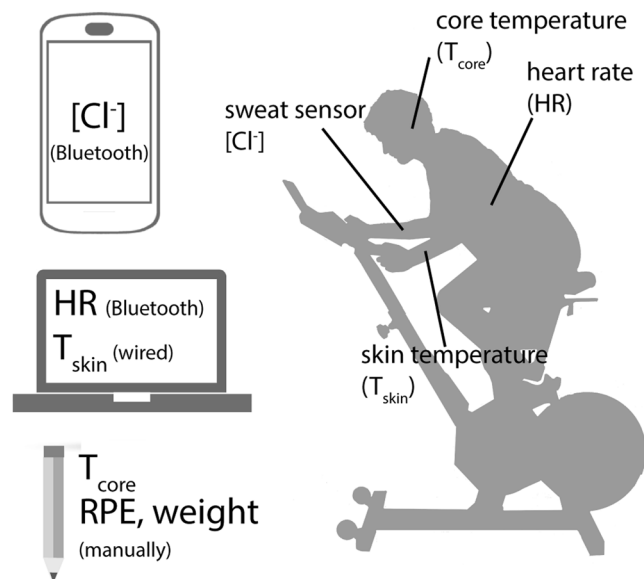


**Figure 2.** On-body trials to measure sweat profile, heart rate, core and skin temperature and weight loss during exercise. The sweat sensor and heart rate sensor were wirelessly (Bluetooth) connected to a smart phone and a laptop and the data were recorded in real time with a 1 Hz sampling rate. The skin temperature ( $T_{skin}$ ) sensor was wired and connected to a laptop, and it was sampled at 2 Hz. The core temperature ( $T_{core}$ ) and RPE values were manually recorded every 5 minutes. The subjects' weight was measured before and after the trial.

(Fig. 3G). The sweat chloride concentrations in the first plateau were in the range of 2.9–34.4 mM ( $11.7 \pm 7.2$  mM, mean  $\pm$  CI) (Fig. 3H). The variation in sweat chloride concentrations could be due to variation in absorption efficiency or sweat rate between individuals. In general, the sweat chloride concentration is thought to increase with increasing sweat rate, however, previous studies have relied on sweat collection over 10–30 minutes and hence the details are not well understood<sup>29–33</sup>. The sweat rate is relatively low at this exercise intensity, and hence the variation is likely due to individual variation in reabsorption. The range of sweat chloride concentrations is consistent with values for healthy individuals following sweat induction by iontophoresis of  $\leq 29$  mM<sup>34</sup>. The methods used for calculation of the onset of sweating and plateau regions are described in detail in *Materials and Methods* and Supplementary Information (Figs. S5 and S6).

**Classification of healthy individuals based on their sweat profile.** In this work, we observed two distinct responses. The Type 1 profile ( $N = 33$ ) was characterized by a single-plateau (slope  $< 0.1$  mM  $\text{min}^{-1}$ ) (Fig. 4A), whereas the Type 2 profile showed multiple-plateaus (Fig. 4B). A single-plateau sweat profile satisfies the condition that the slope is less than  $0.1$  mM  $\text{min}^{-1}$  for the duration of the trial. A multiple-plateau profile had an increase in slope of greater than  $0.1$  mM  $\text{min}^{-1}$  after the first plateau. 14 of the 17 Type 2 profiles had two plateaus, while the remaining three profiles exhibited three plateaus or an increase but no second plateau.

To assess the differences in electrolyte loss between the two groups, we determined the concentration difference ( $\Delta C$ ) between the average chloride ion concentration for the first 10 minutes of the first plateau and the last 10 minutes (75 to 85 minutes) of the trial. The increases in concentration ( $\Delta C$ ) were  $0.6 \pm 1.8$  mM (mean  $\pm$  CI) for Type 1, and  $17.7 \pm 19$  mM for Type 2 (Fig. 4C), clearly showing a difference in physiological response between the two groups ( $p = 0.0012$ ). In addition to differences in  $\Delta C$ , the average chloride ion concentration (at the first plateau) between the two groups was also significantly different:  $9.0 \pm 3.8$  mM for Type 1 and  $16.5 \pm 9.2$  mM for Type 2 ( $p = 0.0038$ ) (Fig. 4D).

The length of the plateau regions was significantly longer for the Type 1 profiles ( $47.0 \pm 7.9$  minutes, mean  $\pm$  CI) compared to the first plateau of the Type 2 profiles ( $15.8 \pm 7.2$  minutes) ( $p < 0.0001$ ), but there was no difference between the lengths of the first plateau of Type 1 and the second plateau of Type 2 profiles (Fig. 4E). In addition, the second plateau of the Type 2 profiles was significantly longer than the corresponding first plateau regions ( $p = 0.00002$ ). There was no difference in the time corresponding to the onset of sweating between the two groups (Fig. 4F).

**Sweat profile and the physiological response.** To assess the relationship between the sweat profile and physiological factors, we analyzed the average heart rate for the last 10 minutes (from 75 to 85 minutes) of the trial ( $HR_{80}$ ), which is the maximum heart rate for all subjects, along with changes in heart rate ( $\Delta HR$ ), RPE ( $\Delta RPE$ ), core ( $\Delta T_{core}$ ) and skin ( $\Delta T_{skin}$ ) temperatures, and body weight ( $\Delta Wgt$ ) (Fig. 5). Individuals with Type 2 profiles had  $HR_{80}$  values of  $132.8 \pm 7.8$  bpm during the trial, which is significantly higher than the value of  $112.4 \pm 5.4$  bpm for Type 1 profiles ( $p = 0.00007$ ) (Fig. 5A). Individuals classified with Type 2 profiles had significantly higher values of  $\Delta HR$ ,  $\Delta Wgt$ , and  $\Delta RPE$  compared to those with Type 1 profiles. For example, individuals with Type 2 profiles had a change in heart rate ( $\Delta HR$ ) of  $15.7 \pm 4.5$  bpm (mean  $\pm$  CI), compared to  $8.0 \pm 2.0$  bpm for Type 1

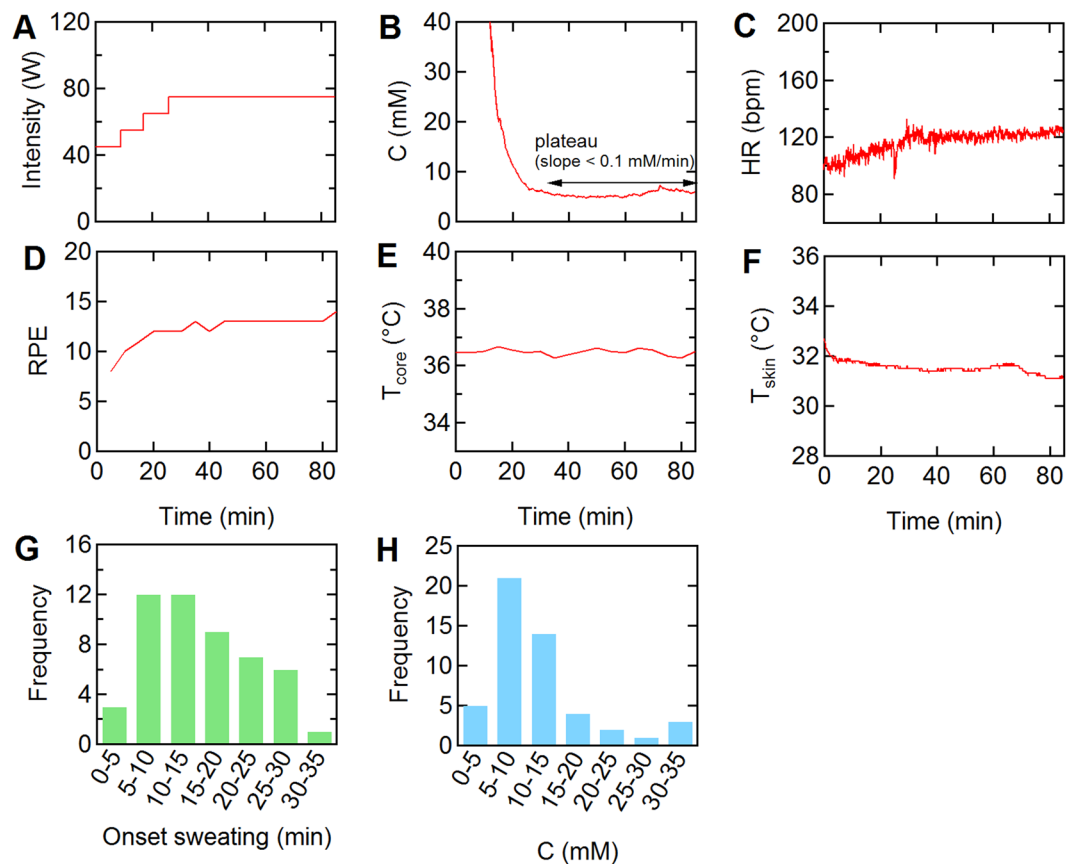


**Figure 3.** Physiological response during 60 minutes spinning at 75 W. Representative physiological measurements. **(A)** Exercise protocol: warm-up: 45 W (8 minutes), 55 W (8 minutes), 65 W (9 minutes), and 75 W (60 minutes). **(B)** Sweat chloride concentration. **(C)** Heart rate (HR). **(D)** Rated perceived exertion (RPE). **(E)** Core temperature ( $T_{\text{core}}$ ) using a tympanic thermometer. **(F)** Skin temperature ( $T_{\text{skin}}$ ) measured on the forearm. **(G)** Distribution of time at the onset of sweating. (from the beginning of the warm-up period). **(H)** Distribution of sweat chloride concentration at the first plateau (see text for details).  $N = 50$ .

profiles ( $p = 0.0053$ ) (Fig. 5B). Individuals with Type 2 profiles had a weight change of  $0.88 \pm 0.10\%$ , compared to  $0.69 \pm 0.05\%$  for Type 1 profiles ( $p = 0.0003$ ).  $\Delta\text{RPE}$  values for individuals with Type 1 and 2 profiles were  $0.9 \pm 0.4$  and  $1.9 \pm 0.5$ , respectively ( $p = 0.0051$ ) (Fig. 5C,D). The difference in core temperature was significantly larger for Type 2 profiles, but was not significant if the outlier was excluded. There was no significant difference in changes in skin temperature. While there was no gender difference in Type 2 individuals, there were significantly fewer females amongst the Type 1 individuals (Fig. 5F).

The physiological responses during exercise are interrelated. To assess the quantitative relationships among the sweat profile and other physiological parameters, principle component analysis (PCA) was performed with 11 variables ( $\Delta C$ ,  $\Delta\text{HR}$ ,  $\Delta\text{RPE}$ ,  $\Delta T_{\text{core}}$ ,  $\Delta T_{\text{skin}}$ ,  $\Delta\text{Wgt}$ , time for onset of sweating, age, exercise frequency, and BMI). The results from this analysis also show the strong correlation among  $\Delta C$ ,  $\Delta\text{Wgt}$ , and  $\Delta\text{HR}$  (Table S1 in Supplementary Information). The eigen value of the first principle component is 22.3%, and the coefficients of  $\Delta\text{Wgt}$ ,  $\Delta C$  and  $\Delta\text{HR}$  were 0.80, 0.65, and 0.77, respectively. Pearson correlation coefficients between  $\Delta C$  and  $\Delta\text{HR}$ ,  $\Delta C$  and  $\Delta\text{Wgt}$ , and  $\Delta\text{HR}$  and  $\Delta\text{Wgt}$  were 0.48, 0.37 and 0.42, respectively (Fig. S7 in Supplementary Information).

**Sweat profiles and exercise intensity.** Since individuals with Type 2 profiles have higher  $\text{HR}_{80}$ ,  $\Delta\text{HR}$ , and  $\Delta\text{RPE}$  values, we can assume that these individuals required a higher level of effort to maintain a power output of 75 W. To assess the influence of level of effort on sweat profile, five subjects with Type 1 sweat profiles performed two additional trials at 100 and 125 W. Figure 6A–C show representative sweat profiles for one subject at the three different exercise intensities. At 75 and 100 W the sweat profiles are Type 1 with a constant sweat chloride during the trial (Fig. 6A,B), however, at 125 W the profile becomes Type 2 (Fig. 6C). During the three trials, the sweat concentrations at the plateau (75 W and 100 W) and the first plateau (125 W) were almost identical (75 W = 14.5 mM, 100 W = 12.3 mM, 125 W = 14.17 mM), but the concentration value at the second plateau during the 125 W trial increased to 23.3 mM. As the exercise intensity increased, the number of Type 2 profiles also increased (Fig. 6D). While all subjects had Type 1 sweat profiles in the 75 W trials, 4 of 5 had Type 2 profiles during the 125 W trials. The change in heart rate for the four subjects with Type 2 profiles at 125 W was larger than the subject with a Type 1 profile, and increased over time during the trial (Fig. 6E,F).

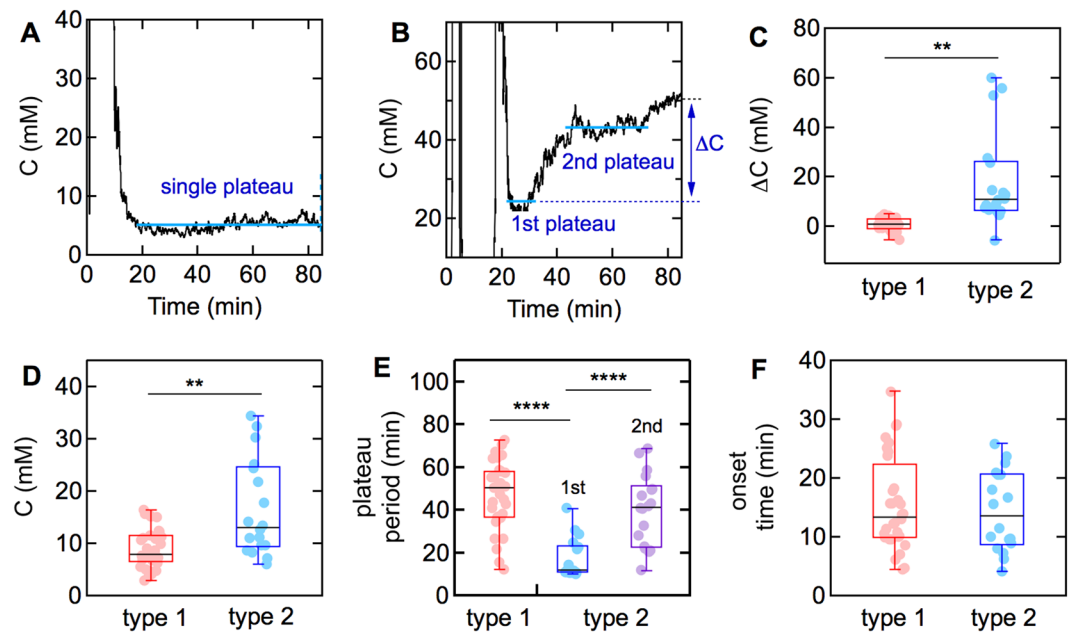


**Figure 4.** Sweat profiles of healthy subjects ( $N = 50$ ) during exercise. **(A)** Representative example of a Type 1 profile with a single plateau. **(B)** Representative example of a Type 2 profile with two plateaus. **(C–F)** Comparison between the two groups with different sweat profiles (Type 1: single plateau, Type 2: multiple plateaus). **(C)** Changes in the sweat concentration during exercise.  $\Delta C = C_2 - C_1$ , where  $C_1$  is the average chloride ion concentration for the first 10 minutes of the first plateau,  $C_2$  is the average chloride ion concentration from 75 to 85 minutes. **(D)** Average sweat chloride ion concentration in the first plateau. **(E)** Plateau period. **(F)** Sweat onset time. \* $p < 0.05$ , \*\* $p < 0.01$ , \*\*\* $p < 0.001$ , \*\*\*\* $p < 0.0001$ .

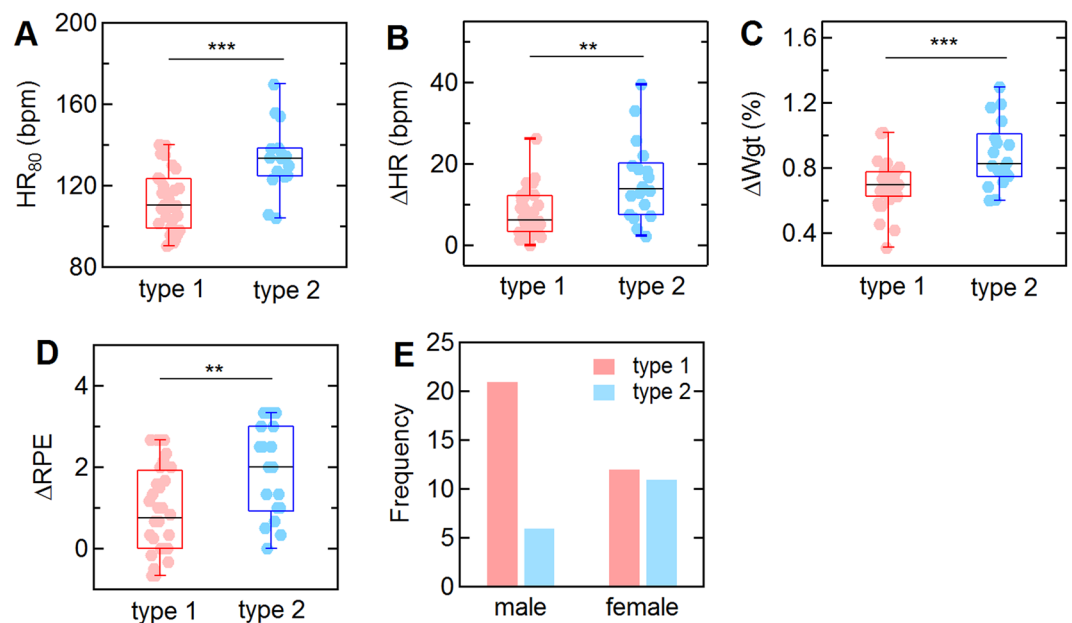


**Figure 5.** Changes in physiological parameters for individuals ( $N = 50$ ) with Type 1 and Type 2 sweat profiles. **(A)** Heart rate averaged for the last 10 minutes (from 75 to 85 minutes) of the trial ( $HR_{80}$ ). **(B)** Change in heart rate ( $\Delta HR$ ). **(C)** Change in body weight ( $\Delta Wgt$ ). **(D)** Change in Rated Perceived Exertion ( $\Delta RPE$ ). **(E)** Gender distribution. Changes in HR were determined from  $\Delta X = X_2 - X_1$ , where  $X_1$  is the average value for the first 10 minutes of the first plateau, and  $X_2$  is the average value from 75 to 85 minutes.  $\Delta Wgt$  was determined from the weight change at the end of the trial normalized to the weight at the beginning of the trial.  $\Delta RPE$  were obtained from the difference in the average values recorded during the first 10 minutes and last 10 minutes at 75 W. \* $p < 0.05$ , \*\* $p < 0.01$ , \*\*\* $p < 0.001$ .

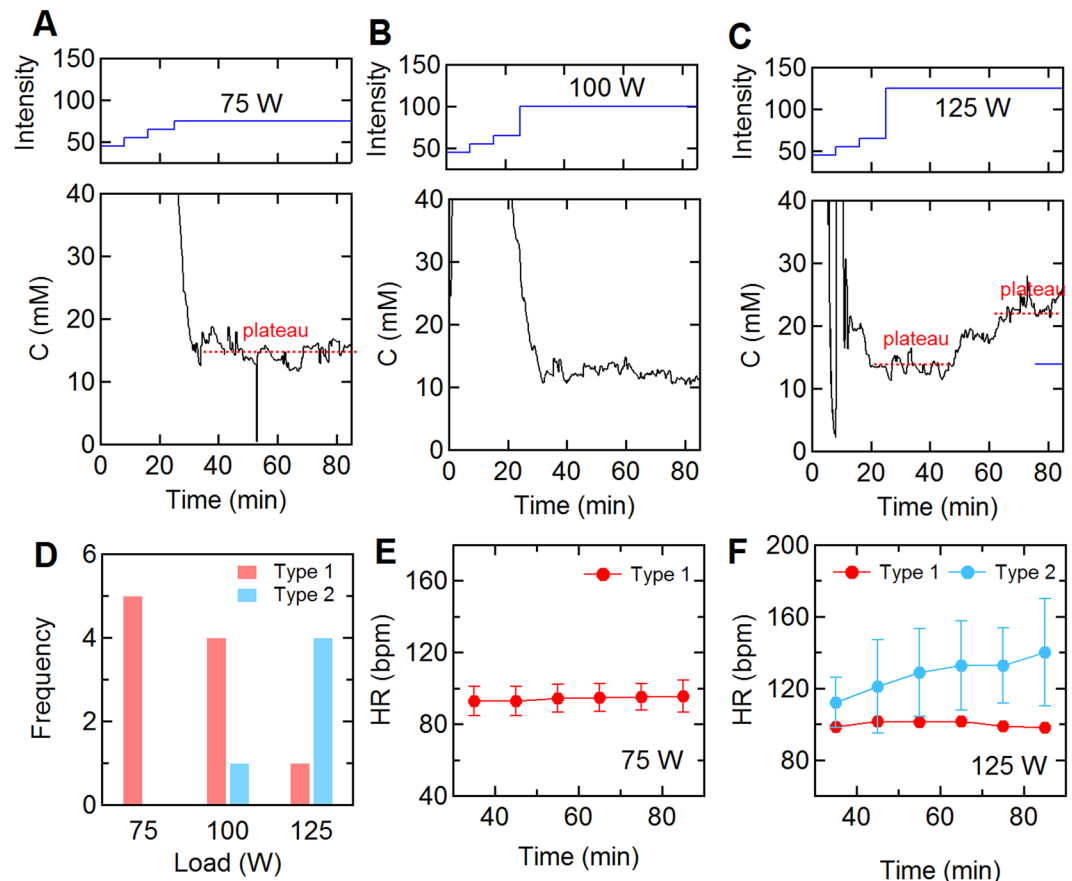


**Figure 6.** Sweat profiles and exercise intensity. (A–C) Sweat profiles for one subject in trials at exercise intensities of (A) 75 W, (B) 100 W, and (C) 125 W. (D) Dependence of sweat profile on exercise intensity. (E,F) Heart rate during (E) 75 W and (F) 125 W trials.

**Prediction model for fluid loss during exertion.** Weight change associated with fluid loss is an important metric for fatigue but is difficult to measure in real time. Since the sweat losses in this study were relatively small ( $<1.5\%$  body weight), they would have no practical physiological impact<sup>35</sup>. However, having demonstrated that the sweat chloride profiles are related to physiological parameters (Fig. 4 and Table S1 in Supplementary Information), we next created a prediction model to classify subjects according to their weight loss during exercise. For classification we set the weight loss cut-off to the median value:  $0.74\%$  bodyweight (group 1:  $\Delta Wgt < 0.74\%$ , group 2:  $\Delta Wgt > 0.74\%$ ). We employed a random forest method<sup>36</sup> using  $\Delta C$ ,  $\Delta HR$ ,  $\Delta T_{core}$ ,  $\Delta RPE$ , onset time, exercise frequency, BMI, and gender as independent variables.

Two metrics commonly used to evaluate the performance of random forest models are the out-of-bag (OOB) error and the AUC (area under the ROC curve, 1: perfect classification, 0.5: no better than random classification). The OOB error, an estimation of the true prediction error, was  $32\%$  (group 1:  $28\%$  (7/25), group 2:  $36\%$  (9/25)) and the AUC value was  $0.742$  (Fig. 7A). Interestingly, the sweat chloride concentration was the most effective variable contributing to the classification (Fig. 7B). Although a few previous studies have reported that hydration status can be classified or estimated by monitoring physiological parameters or by analyzing biofluids, these studies used *post hoc* laboratory-based analytical measurements<sup>37–39</sup>. Here we show that chloride ion concentration and other physiological parameters recorded using wearable devices can be used to predict fluid loss due to sweating.

## Conclusions

Wearable sensors provide new opportunities for monitoring an individual's health state. While most wearable sensors measure physiological parameters such as heart rate, activity, and skin temperature, the development of wearable sensors for biological analytes has been more challenging. Sensors that measure the electrolyte concentration in sweat can provide new insight into time-dependent changes in health state relevant to human performance, heat exertion, and electrolyte imbalance disorders. In this work, sweat profiles were recorded at a constant moderate exercise load ( $N = 65$ ). The 65 wearable sensors used in this study had a slope of  $-53.6 \pm 3.5$  mV/decade and y-intercept of  $174.4 \pm 12.9$  mV in the measured calibration curves. Here we show that the real-time chloride ion concentration in sweat can reflect each individual's physiological response during exercise. Using sweat profile measured by the wearable sensor, we could classify individuals into two groups with significant different changes in heart rate, RPE, and weight losses during 1 hour of exercise at 75 W of intensity. Finally, we showed that sweat profiles along with other physiological signals can be used to predict fluid loss with out of bag



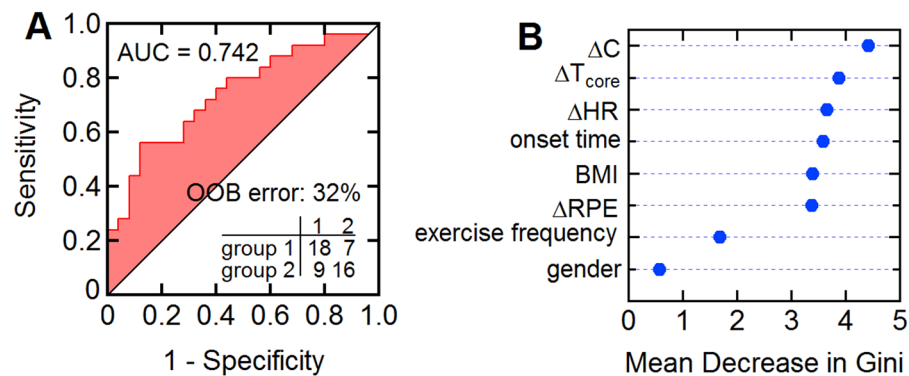


**Figure 7.** Predictive model to classify dehydration status. (A) OOB (out-of-bag) error, ROC (receiver operating characteristic) curve, and AUC (area under ROC curve). Sensitivity: probability that the prediction result will be group 1 when  $\Delta Wgt < 0.74\%$ . Specificity: probability that the prediction result will be group 2 when  $\Delta Wgt > 0.74\%$ . (B) Mean decrease in Gini coefficient (a higher value indicates more important variable).

(OOB) error and AUC values were 32% and 0.74, respectively. These results suggest that sweat sensors could provide real-time feedback on a range of parameters associated with exercise and exertion and enable data-driven fluid intake schedules.

## Materials and Methods

**Sweat sensor.** The wearable sweat chloride sensor used in this work consists of two Ag/AgCl electrodes and a salt bridge (Fig. S2A–D in Supplementary Information). Prior to each trial, all sensors were calibrated using 10, 50, and 100 mM NaCl solution at room temperature (Fig. S2E in Supplementary Information). The calibration curves were then adjusted to skin temperature using the Nernst equation. The integrated salt bridge minimizes the equilibrium between the reference hydrogel and sweat sample, which enables accurate measurement of sweat chloride concentration for an extended period of more than 12 hours (Fig. S2F in Supplementary Information)<sup>9,11</sup>. In addition, the sensor has a response time of 2 s in the concentration range from 10 to 150 mM<sup>11</sup>. The mean difference between sweat chloride concentrations measured by the sweat sensor and the standard method used in cystic fibrosis clinics was  $6.2 \pm 9.5$  mM, which is close to the arm-to-arm physiological variation of about 3 mM<sup>10</sup>. The correlation coefficient between the sensor and laboratory measurement was 0.97.

**On-body trials.** All on-body trials were performed under a protocol approved by the institute review board (IRB) at Johns Hopkins University (IRB00122647). All experiments were performed in accordance with guidelines and regulations. All participants provided written informed consent before participation. Participants read the study participation informative document and signed the corresponding informed consent. 50 subjects participated in this study and their personal information including age, gender, height, weight, medical history and exercise habits were recorded (see Fig. S1 in Supplementary Information). Subjects did not consume food or water in the 3 hours before the start of the trial, and 5 mL per kg bodyweight of water was provided before the start of each trial. Identical T-shirts and shorts were provided to all subjects for the trial. All trials involved spinning on a stationary bike (LifeCycle 9500HR, Life Fitness). In this work, the exercise protocol was designed for all subjects to maintain prolonged spinning during the entire protocol, regardless of their gender, age and fitness level. Subjects warmed up by spinning at three graded exercise intensities for 25 minutes (45 W for 8 minutes, 55 W for 8 minutes, 65 W for 9 minutes). After the warm-up, subjects increased the exercise intensity to 75 W for 60 minutes. During the trials, the subjects did not consume any food or water. Room temperature was maintained at 25 °C.

During the trials, the sweat chloride concentration, heart rate, and core and skin temperatures were measured using various sensors, and the rated perceived exertion (RPE, Borg scale) was monitored by self-reporting (Fig. 2). The sweat chloride sensor was attached to a forearm using a commercial bandage (Tegaderm, 3 M) and the real-time output was monitored at a sampling frequency of 1 Hz by a Bluetooth wireless transceiver and a mobile app<sup>10</sup>. A heart rate monitor (Zephyr Bio Harness, Medtronic) and a thermocouple sensor (ThermoScientific, NeuLog) were employed to measure the heart rate and the skin temperature, respectively. RPE and core (tympanic) temperature values were recorded every 5 minutes. The weight change before and after the trial was measured without clothing and after removing all sweat from the body, using a conventional scale (HBF-514C, Omron, 0.1 kg resolution).

**Sweat profile analysis.** The onset time for sweating was obtained by monitoring the change in electrical noise of the sweat sensor output, which decreased when the space between the sensor and the skin was filled with sweat. Here we define the onset time for sweating as the time when the standard deviation (SD) of the sensor signal was smaller than 50 mM over for 30 s (see Fig. S5 in Supplementary Information).

A plateau region in a measured sweat profile was defined as when the slope was smaller than  $0.1 \text{ mM min}^{-1}$  for at least 10 minutes (Fig. S6 in Supplementary Information). To find a plateau region, a sequential linear regression (least squares fit) was performed by applying a moving 10-minute time window. The time window was advanced in 1-second increments. The start of a plateau is the start of the first 10 minute period where the slope is

$<0.1 \text{ mM min}^{-1}$ , and the end of the plateau is the time where the slope exceeds  $0.1 \text{ mM min}^{-1}$ . If a single plateau extended to the end of the trial, the profile was designated Type 1. Profiles were also designated as Type 1 if they exhibited two plateaus with less than 5 mM difference. Sweat profiles with two or three plateaus (with  $>5 \text{ mM}$  difference), or a single plateau followed by an increase were designated as Type 2. A customized code to identify plateau regions was developed using MATLAB.

**Statistical analysis and machine learning.** Statistical analysis was performed using R and SPSS software (IBM). After classifying the subjects into two groups based on their sweat profiles, a student's t-test was performed to calculate the statistical significance between physiological parameters. Principle component analysis (PCA) was performed to interpret complex relations among the numerous measured physiological signals. Finally, a random forest algorithm was employed to develop a predictive model to classify the subjects according to their weight loss.

Received: 26 July 2019; Accepted: 7 November 2019;

Published online: 29 November 2019

## References

- Schwellnus, M. P. Cause of exercise associated muscle cramps (EAMC)—altered neuromuscular control, dehydration or electrolyte depletion? *Br J Sports Med* **43**, 401–408, <https://doi.org/10.1136/bjism.2008.050401> (2009).
- Bigard, A. X. *et al.* Effects of dehydration and rehydration on EMG changes during fatiguing contractions. *Med Sci Sports Exerc* **33**, 1694–1700 (2001).
- Clarkson, P. M. & Haymes, E. M. Exercise and mineral status of athletes: calcium, magnesium, phosphorus, and iron. *Med Sci Sports Exerc* **27**, 831–843 (1995).
- Vanderghyest, F. *et al.* Impact of hyponatremia on nerve conduction and muscle strength. *Eur J Clin Invest* **46**, 328–333, <https://doi.org/10.1111/eci.12597> (2016).
- Sawka, M. N. *et al.* American College of Sports Medicine position stand. Exercise and fluid replacement. *Med Sci Sports Exerc* **39**, 377–390, <https://doi.org/10.1249/mss.0b013e31802ca597> (2007).
- Sawka, M. N., Cheuvront, S. N. & Kenefick, R. W. Hypohydration and Human Performance: Impact of Environment and Physiological Mechanisms. *Sports Med* **45**(Suppl 1), S51–60, <https://doi.org/10.1007/s40279-015-0395-7> (2015).
- Glaser, J. *et al.* Climate Change and the Emergent Epidemic of CKD from Heat Stress in Rural Communities: The Case for Heat Stress Nephropathy. *Clin J Am Soc Nephrol* **11**, 1472–1483, <https://doi.org/10.2215/CJN.13841215> (2016).
- Nerbass, F. B. *et al.* Occupational Heat Stress and Kidney Health: From Farms to Factories. *Kidney Int Rep* **2**, 998–1008, <https://doi.org/10.1016/j.ekir.2017.08.012> (2017).
- Choi, D. H., Kim, J. S., Cutting, G. R. & Searson, P. C. Wearable Potentiometric Chloride Sweat Sensor: The Critical Role of the Salt Bridge. *Anal Chem* **88**, 12241–12247, <https://doi.org/10.1021/acs.analchem.6b03391> (2016).
- Choi, D. H. *et al.* Sweat test for cystic fibrosis: Wearable sweat sensor vs. standard laboratory test. *J Cyst Fibros* **17**, e35–e38, <https://doi.org/10.1016/j.jcf.2018.03.005> (2018).
- Choi, D. H., Li, Y., Cutting, G. R. & Searson, P. C. A wearable potentiometric sensor with integrated salt bridge for sweat chloride measurement. *Sensors and Actuators B-Chemical* **250**, 673–678 (2017).
- Rose, D. P. *et al.* Adhesive RFID Sensor Patch for Monitoring of Sweat Electrolytes. *IEEE Trans Biomed Eng* **62**, 1457–1465, <https://doi.org/10.1109/TBME.2014.2369991> (2015).
- Gao, W. *et al.* Fully integrated wearable sensor arrays for multiplexed *in situ* perspiration analysis. *Nature* **529**, 509–514, <https://doi.org/10.1038/nature16521> (2016).
- Alizadeh, A. *et al.* A wearable patch for continuous monitoring of sweat electrolytes during exertion. *Lab Chip* **18**, 2632–2641, <https://doi.org/10.1039/c8lc00510a> (2018).
- Koh, A. *et al.* A soft, wearable microfluidic device for the capture, storage, and colorimetric sensing of sweat. *Sci Transl Med* **8**, 366ra165, <https://doi.org/10.1126/scitranslmed.aaf2593> (2016).
- Guinovart, T., Bhandodkar, A. J., Windmiller, J. R., Andrade, F. J. & Wang, J. A potentiometric tattoo sensor for monitoring ammonium in sweat. *Analyst* **138**, 7031–7038, <https://doi.org/10.1039/c3an01672b> (2013).
- Bhandodkar, A. J. *et al.* Epidermal tattoo potentiometric sodium sensors with wireless signal transduction for continuous non-invasive sweat monitoring. *Biosens Bioelectron* **54**, 603–609, <https://doi.org/10.1016/j.bios.2013.11.039> (2014).
- Coyle, S. *et al.* BIOTEX—biosensing textiles for personalised healthcare management. *IEEE Trans Inf Technol Biomed* **14**, 364–370, <https://doi.org/10.1109/TITB.2009.2038484> (2010).
- Boysen, T. C., Yanagawa, S., Sato, F. & Sato, K. A modified anaerobic method of sweat collection. *J Appl Physiol Respir Environ Exerc Physiol* **56**, 1302–1307, <https://doi.org/10.1152/jappp.1984.56.5.1302> (1984).
- Buono, M. J., Lee, N. V. & Miller, P. W. The relationship between exercise intensity and the sweat lactate excretion rate. *J Physiol Sci* **60**, 103–107, <https://doi.org/10.1007/s12576-009-0073-3> (2010).
- Stofan, J. R. *et al.* Sweat and sodium losses in NCAA football players: a precursor to heat cramps? *Int J Sport Nutr Exerc Metab* **15**, 641–652 (2005).
- Casa, D. J. *et al.* National athletic trainers' association position statement: fluid replacement for athletes. *J Athl Train* **35**, 212–224 (2000).
- Vrijens, D. M. & Rehrer, N. J. Sodium-free fluid ingestion decreases plasma sodium during exercise in the heat. *J Appl Physiol* (1985) **86**, 1847–1851, <https://doi.org/10.1152/jappp.1999.86.6.1847> (1999).
- Hawley, J. A., Dennis, S. C. & Noakes, T. D. Carbohydrate, fluid, and electrolyte requirements of the soccer player: a review. *Int J Sport Nutr* **4**, 221–236 (1994).
- Mora-Rodríguez, R. Influence of aerobic fitness on thermoregulation during exercise in the heat. *Exerc Sport Sci Rev* **40**, 79–87, <https://doi.org/10.1097/JES.0b013e318246ee56> (2012).
- Periard, J. D., Travers, G. J. S., Racinais, S. & Sawka, M. N. Cardiovascular adaptations supporting human exercise-heat acclimation. *Auton Neurosci* **196**, 52–62, <https://doi.org/10.1016/j.autneu.2016.02.002> (2016).
- Mora-Rodríguez, R., Del Coso, J., Hamouti, N., Estevez, E. & Ortega, J. F. Aerobically trained individuals have greater increases in rectal temperature than untrained ones during exercise in the heat at similar relative intensities. *Eur J Appl Physiol* **109**, 973–981 (2010).
- Fernandes, A. D. *et al.* Measuring skin temperature before, during and after exercise: a comparison of thermocouples and infrared thermography. *Physiol Meas* **35**, 189–203, <https://doi.org/10.1088/0967-3334/35/2/189> (2014).
- Bijman, J. & Quinton, P. M. Influence of abnormal Cl<sup>-</sup> impermeability on sweating in cystic fibrosis. *Am J Physiol* **247**, C3–9, <https://doi.org/10.1152/ajpcell.1984.247.1.C3> (1984).
- Emrich, H. M. *et al.* Sweat composition in relation to rate of sweating in patients with cystic fibrosis of the pancreas. *Pediatr Res* **2**, 464–478, <https://doi.org/10.1203/00006450-196811000-00004> (1968).



31. Sonner, Z. *et al.* The microfluidics of the eccrine sweat gland, including biomarker partitioning, transport, and biosensing implications. *Biomicrofluidics* **9**, 031301, <https://doi.org/10.1063/1.4921039> (2015).
32. Buono, M. J., Ball, K. D. & Kolkhorst, F. W. Sodium ion concentration vs. sweat rate relationship in humans. *J Appl Physiol* **103**, 990–994, <https://doi.org/10.1152/jappphysiol.00015.2007> (2007).
33. Buono, M. J., Claros, R., DeBoer, T. & Wong, J. Na<sup>+</sup> secretion rate increases proportionally more than the Na<sup>+</sup> reabsorption rate with increases in sweat rate. *J Appl Physiol* **105**, 1044–1048, <https://doi.org/10.1152/jappphysiol.90503.2008> (2008).
34. Farrell, P. M. *et al.* Diagnosis of Cystic Fibrosis: Consensus Guidelines from the Cystic Fibrosis Foundation. *J Pediatr* **181S**, S4–S15 e11, <https://doi.org/10.1016/j.jpeds.2016.09.064> (2017).
35. Sawka, M. N. & Noakes, T. D. Does dehydration impair exercise performance? *Med Sci Sports Exerc* **39**, 1209–1217, <https://doi.org/10.1249/mss.0b013e318124a664> (2007).
36. Breiman, L. Random forests. *Machine Learning* **45**, 5–32, <https://doi.org/10.1023/A:1010933404324> (2001).
37. Ring, M., Lohmueller, C., Rauh, M. & Eskofier, B. M. On Sweat Analysis for Quantitative Estimation of Dehydration during Physical Exercise. *2015 37th Annual International Conference of the IEEE Engineering in Medicine and Biology Society (Embc)*, 7011–7014 (2015).
38. Ring, M., Lohmueller, C., Rauh, M., Mester, J. & Eskofier, B. M. Salivary Markers for Quantitative Dehydration Estimation During Physical Exercise. *Ieee Journal of Biomedical and Health Informatics* **21**, 1306–1314, <https://doi.org/10.1109/jbhi.2016.2598854> (2017).
39. Kaveh, A. & Chung, W. Classification of Hydration Status Using Electrocardiogram and Machine Learning. *2013 International Symposium on Computational Models for Life Sciences* **1559**, 240–249 <https://doi.org/10.1063/1.4825016> (2013).

## Acknowledgements

This work was supported in part by the Cystic Fibrosis Foundation (grants SEARSO6XX0 and SEARSO18K0). The authors would like to thank Under Armor that donated t-shirts and shorts for on-body trials.

## Author contributions

D.H.C. and P.C.S. designed the study. D.H.C., G.K., Y.L., K.K. and J.N. performed the trials and collected the data. D.H.C., J.K. and S.L.Z. performed the statistical analysis. I.C.J. contributed to the design of the exercise protocol. D.H.C. and K.J.S. contributed to physiological interpretation of the data. D.H.C. and P.C.S. wrote the manuscript. All authors read and approved the final manuscript.

## Competing interests

The authors declare no competing interests.

## Additional information

**Supplementary information** is available for this paper at <https://doi.org/10.1038/s41598-019-54202-1>.

**Correspondence** and requests for materials should be addressed to P.C.S.

**Reprints and permissions information** is available at [www.nature.com/reprints](http://www.nature.com/reprints).

**Publisher's note** Springer Nature remains neutral with regard to jurisdictional claims in published maps and institutional affiliations.



**Open Access** This article is licensed under a Creative Commons Attribution 4.0 International License, which permits use, sharing, adaptation, distribution and reproduction in any medium or format, as long as you give appropriate credit to the original author(s) and the source, provide a link to the Creative Commons license, and indicate if changes were made. The images or other third party material in this article are included in the article's Creative Commons license, unless indicated otherwise in a credit line to the material. If material is not included in the article's Creative Commons license and your intended use is not permitted by statutory regulation or exceeds the permitted use, you will need to obtain permission directly from the copyright holder. To view a copy of this license, visit <http://creativecommons.org/licenses/by/4.0/>.

© The Author(s) 2019